Biomass steam gasification in fluidized bed of inert or catalytic particles: Comparison between experimental results and thermodynamic equilibrium predictions

M. Detournay *, M. Hemati, R. Andreux

Laboratoire de Génie Chimique de Toulouse, Institut National Polytechnique de Toulouse, 4 Allée Emile Monso BP 44362, 31432 Toulouse Cedex 4, France

A B S T R A C T

In order to improve the understanding of biomass gasification in a bed fluidized by steam, the thermochemical equilibrium of the reactive system was studied. The equilibrium results were compared to LGC experimental results, obtained by the gasification of oak and fir in a laboratory-scale fluidized bed of different catalysts: sand, alumina, and alumina impregnated with nickel.
The research was completed by a study of the influence on the equilibrium of additional parameters such as the quantity of steam, the pressure or the kind of biomass. Those results of simulation may be used for evaluating the limits of actual reactors.
The following conclusion may be drawn from all the results:

The thermodynamic equilibrium state calculated is far away from the experimental results obtained on sand particles.
The steam to biomass ratio, between 0.4 and 1 $kg_{steam}/kg_{dry\ biomass}$, has a strong influence on the gas mixture composition.
The temperature increase and the use of catalyst allow producing a gas mixture with a high content of hydrogen and carbon monoxide. The H_2:CO ratio may reach values greater than 3.
The use of catalyst allows the system to get closer from the equilibrium, especially for the nickel based catalyst.

1. Introduction

Due to growing environmental concern, biomass utilization for power generation has increased. If the conversion of biomass may lead to electricity *via* gas engines or gas turbines, an increasing interest has been showed to substitution fuels synthesis from biomass steam gasification, such as methanation and "Biomass To Fischer–Tropsch Liquids". For those processes, the gas produced by gasification, called syngas, has to meet the following specifications: low quantity of inert gases, low sulfur content (< 0.1 ppm), H_2:CO ratio close from the expected synthesis reactions stoechiometric ratio (2 for Fischer–Tropsch, 3 for methanation).

The air-blown gasification process is almost rejected by those specifications.

Biomass steam gasification in several steps (Fig. 1):

- At temperatures greater than 350 °C, biomass is converted into volatiles products which are either condensable (steam and tars) or incondensable (H_2, CO, CO_2, CH_4, C_2H_4, C_2H_6 and light hydrocarbons). This reaction is the pyrolysis and also leads to a carbonated residue called char.
- The char then reacts with steam (Eq. (1)) above 600 °C. This reaction is extremely fast at temperatures greater than 850 °C. The char also reacts with the gases produced by the pyrolysis: with carbon dioxide in Boudouard reaction (Eq. (2)), and with hydrogen in reaction (Eq. (3)).

$$C + H_2O = CO + H_2 \qquad \Delta H_r^0 = 131.3 kJ/mol \tag{1}$$

$$C + CO_2 = 2CO \quad \Delta H_r^0 = 172.4 kJ/mol \tag{2}$$

$$C + 2H_2 \quad \Delta H_r^0 = -74.6 kJ/mol \tag{3}$$

- Above 650 °C, tars react with steam in cracking and reforming reactions. Steam also reacts with incondensable gases: methanation reaction (Eq. (4)) and water–gas shift reaction (Eq. (5)).

$$CO + 3H_2 = CH_4 + H_2O \quad \Delta H_r^0 = -206.1 kJ/mol \tag{4}$$

$$CO + H_2O = CO_2 + H_2 \quad \Delta H_r^0 = -41.1 kJ/mol \tag{5}$$

The reactive system of biomass conversion (pyrolysis + gasification) is globally endothermic: approximately 52 $kJ/k_{moldry\ biomass}$. A contribution of energy is thus necessary in order to bring the gasification agents up to temperature and to maintain those reactions. This contribution is either given by combustion of biomass, char and gases

* Corresponding author. Tel.: +33 5 34 32 36 93; fax: +33 5 34 32 37 00.
E-mail addresses: marc.detournay@ensiacet.fr (M. Detournay), mehrdji.hemati@ensiacet.fr (M. Hemati).

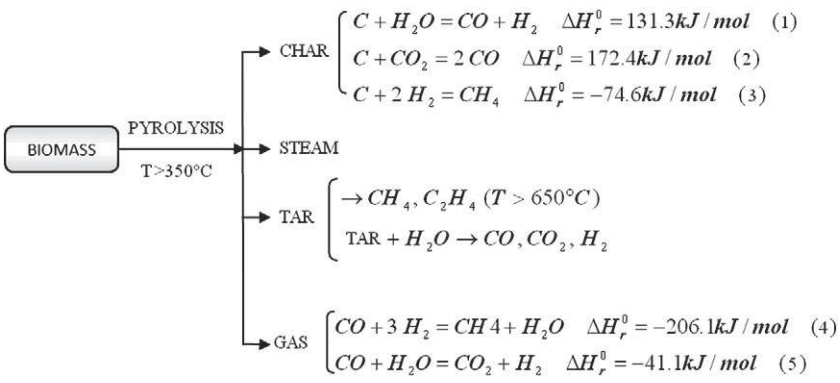

Fig. 1. Synthesis of the reactions happening during biomass steam gasification.

in oxygen and steam gasification processes (where the fluidizing agent is a mixture of oxygen and steam) or from an external source in steam gasification processes. Concerning the latter, energy is often introduced thanks to solid heat carrier particles. There are three kinds of gasifiers, classified depending on the way biomass and gases meet: fixed beds (moving with gravity), trained beds and fluidized beds. Among those three groups, fluidized beds have shown to be the most interesting, for both oxysteam gasification and steam gasification. The most interesting characteristics are an easy control of temperature, an excellent heat transfer between reactors main areas, an easy solid handling and a good contact between solid and gas reactants.

Several processes have been developed on the basis of those advantages: process from Batelle Columbus (MSFBG), LTH, Battelle Memorial Institute [1–3] and more recently the Fast Internally Circulating Fluidized Bed (FICFB) developed by REPOTEC company, in Güssing, Austria [4,5] (Fig. 2). The principle of those processes consists in heating the fluidizing media (sand, olivine or catalyst particles) in a separated reactor, and then to recycle it when heated in the gasification reactor. The necessary energy is furnished by the combustion of a part of the char produced by steam gasification.

In order to design this kind of process, models have been studied. To allow an important number of simulations in a short amount of time, thermochemical equilibrium was first introduced by Gumz [6] and has then often been used to model gasifiers operation [7–15]. This is a constrain optimisation problem, based either on a Gibbs Free energy minimization or on equilibrium constants [7]. Comparison of the theoretical results with the experimental data have been realized mainly for downdraft gasifiers [8–11], for coal gasification [12,13], and most often for air-blown gasifiers [9–12,14]. The work of Schuster and al. [15] has focused on biomass steam gasification and have concluded that the accuracy of the equilibrium model elaborated is sufficient for thermodynamic considerations. The literature review shows that the results given by thermochemical equilibrium approach may not be of an high accuracy. The gap between experimental and equilibrium data has been supposed to be inevitable, especially because of temperatures lower than 800 °C, for which the equilibrium state is not possible [11]. However, some trends may be isolated, and satisfactory results may be observed depending on process and operating conditions. Finally, authors agree to consider the thermochemical equilibrium models results as a limit for gasification systems, since gasification reactions are limited by kinetics [16].

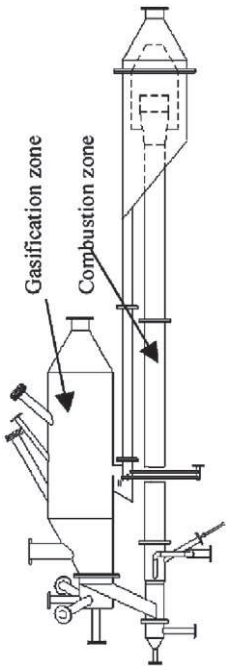

Fig. 2. Reaction unit of the FICFG Güssing gasifier.

In this work, the thermochemical equilibrium has been studied in an air free atmosphere of steam. The results have first been analyzed to figure out the relative importance of reactions involved in steam gasification. The comparison with experimental data has been made with results from the Toulouse Chemical Engineering Laboratory (Laboratoire de Génie Chimique de Toulouse), in which biomass (wood) pyrolysis and gasification has been studied in fluidized beds of different fluidizing media (sand, alumina, and Ni/alumina catalyst) [17,18].

This comparison has shown that the thermodynamic equilibrium can be considered as a limit for the experimental results, and that the use of catalyst allows reaching a state close from the thermodynamic equilibrium state in a short amount of time. The effect of low temperatures on the system efficiency may thus be corrected by appropriate choice of fluidizing media and process parameters.

1.1. Studied parameters

The following parameters have been studied:

- Steam gasification reactor temperature.
- Steam partial pressure in the reactor. It depends on the biomass composition, on its moisture content, and of the steam to biomass ratio X_{vap}. X_{vap} is defined as the ratio between the mass of steam and the mass of dry biomass introduced in the reactor.
- Reactor pressure.
- Kind of biomass.
- Kind of fluidizing media. This parameter impacts exclusively on experimental results.

1.2. Studied criteria

Results have been analyzed thanks to the following criteria:

- Molar fractions of dry and wet incondensable gas mixture (x_i fraction of component i).

- Gasification rate X_g, defined as the ratio between the number of moles of carbon in the incondensable gas mixture and the number of moles of carbon in the biomass introduced in the reactor.
- Char rate X_s, defined as the ratio between the number of moles of carbon in the carbonated residue (char) and the number of moles of carbon in the biomass introduced in the reactor.
- Energy recovery rate R_e, defined as the ratio between the energy which can be recovered in incondensable gas mixture produced by the steam gasification of one kilogram of dry biomass, and the energy produced by the combustion of the same amount of biomass.
- Gasification ratio R_g, defined as the mass of the incondensable gas mixture produced by the steam gasification of one kilogram of dry biomass.
- Molar H_2:CO ratio. The expected value may vary according the syngas industrial goal. For methanation, this ratio has to be close from 3, yet in methanol synthesis (Eq. (6)) or Fischer–Tropsch liquids (Eq. (7)), it has to be close from 2:

$$\text{Methanation}: CO + 3H_2 = CH_4 + H_2O \quad (4)$$

$$\text{Methanol synthesis}: 2H_2 + CO = CH_3OH \quad (6)$$

$$\text{Fischer}-\text{Tropsch liquids}: (2n+1)H_2 + n\ CO = C_nH_{2n+2} + n\ H_2O \quad (7)$$

2. Tools

2.1. Experimental tool

Experiments have been realized with wood sawdust, sieved to obtain a distribution between 300 and 450 μm. It is first drought to moisture content around 4% (mass), and then introduced continuously in the reactor through a worm drive. The reactor is an NS-30 stainless steel shell (thickness: 1.5 mm; width: 150 mm; height: 400 mm). It is provided with a perforated plate distributor with a porosity of 1.82%. The pilot is placed in a cylindrical oven able to deliver a power of 4700 W. The working temperature is the bed temperature, which has been previously checked to be homogeneous in the whole bed.

The produced gases go firstly through a cyclone, then through two water coolers ensuring water and tar condensation. A fraction of the gas is separated at the coolers outlet, then filtered and drought before being analyzed on two chromatography columns: a Porapack column allowing the separation of CO_2, C_2H_4 and C_2H_6, and a molecular sieve allowing the separation of H_2, N_2, CH_4 and CO.

Both reactive and analytical systems have been completely described in [17,18].

2.2. Theoretical tool

The thermodynamic equilibrium calculations have been realized with HSC Chemistry 5.1 software, based on Gibbs Energy MINImization (GEMINI code). For a closed system of N components, the Gibbs energy is expressed according to Eq. (8):

$$G = \sum_{i=1}^{N} n_i \left(\mu_i^0 + RT\ln(a_i)\right) \quad (8)$$

With n_i number of moles of component i in the system, μ_i component i standard chemical potential, a_i component i activity.

The software takes into account the possibility of several phases' coexistence. In our case, the gas phase is composed by the mixture of condensable and incondensable gases, and the solid phase by the carbonated residue. The most stable form of solid carbon is evaluated by the Gibbs energy minimization.

The simulations have been conducted with the following protocol:

- Choice of the existing elements in the system initial state (carbon, hydrogen, oxygen).
- Evaluation of the products stability. The thermodynamic equilibrium has been simulated by considering an exhaustive group of the possible products obtained by a combination of the elements just cited. Results have shown that only nine products are present at the thermodynamic equilibrium state (molar fraction>10–8%): C(s), H_2O(g), H_2(g), CO(g), CO_2(g), CH_4(g), C_2H_4(g), C_2H_6(g) and C_6H_6(g). The molar fraction obtained concerning C_2H_4(g), C_2H_6(g) and C_6H_6(g) have not been greater than 0.1% in any of the simulated cases. Since this study is not dedicated to minority components, they will not be presented in the whole theoretical part of equilibrium calculations.
- Evaluation of studied parameters (see above) influence on the thermodynamic equilibrium.

3. Studied conditions

The results obtained within our laboratory are related with temperature influence on wood gasification in fluidized beds of three kinds of materials: sand particles, alumina particles, and Nickel catalyst on alumina particles. The latter has been prepared by treating alumina particles by activating them with a Nickel nitrate solution, and then calcinated in a fluidized bed [17]. The different conditions applied in the tests are gathered in Table 1.

In order to study the pyrolysis (tests X1 and X5), the reactor had to be fluidized without any water. Nitrogen has been used instead of steam.

The experiments results have been compared to simulation results in the same conditions. The conditions for each run are gathered in Table 2.

4. Comparison between experimental and theoretical rsults

4.1. Pyrolysis ($X_{vap} = 0 kg_{steam}/kg_{dry\ biomass}$)

The comparison between oak pyrolysis experiments and simulations (X1 and S1) are presented in Figs. 3–5.

4.1.1. Gasification rate and gasification ratio

Fig. 3 shows that experimental gasification rate (X_g) and gasification ratio (R_g) have the same evolution than the predicted equilibrium. The gap between theoretical and experimental gasification rate decreases when the temperature increases (the difference is 10% at 700 and 800 °C, and becomes null at 900 °C). The cracking of tar, producing lighter gases, may explain this observation since it is promoted by temperature raise.

Above 900 °C, the temperature does not have any effect on theoretical gasification rate, gasification ratio and char rate.

The experimental results of Fig. 4 show that the temperature has a small influence on the actual composition of the syngas, especially for temperatures above 800 °C. Yet tar cracking is promoted by temperature increase, its impact on gas composition remains low.

The H_2 actual fraction is four times lower than the theoretical equilibrium value, whereas CH_4, CO_2 and C_2H_4 actual fractions are greater than the equilibrium results. Some of the light hydrocarbons (CH_4, C_2H_4, C_2H_6) may not have been converted enough during the experiments. This therefore means that condensable and incondensable gases residence time May have been too short to get as close as possible from the thermodynamic equilibrium state.

H_2: CO ratio is shown in Fig. 3b. We can point out that its real evolution versus temperature is low (from 0.4 to 0.5), yet the influence of temperature is really important for the equilibrium

Table 1
Tests conditions.

Test	Fluidizing media	Kind of biomass	Biomass flowrate, Q_b (g/h)	Particles diameter, dp (μm)	Reactor temperature, T (°C)	Steam rate, X_{vap} ($kg_{steam}/kg_{biomass}$)	Fluidizing gas flowrate, Q (m^3/h)
X1	Sand	Oak:$CH_{1.36}O_{0.67}$	145	315–400	700–950	0 (pyrolysis)	1.14 (N_2)
X2	Sand		600	315–400	700–900	1	1.2 (H_2O)
X3	Alumina			325–400	700–900	1	1.2 (H_2O)
X4	Ni/Alumina			315–500	700–850	1	1.2 (H_2O)
X5	Sand	Fir:$CH_{1.45}O_{0.67}$	145	315–400	850–980	0 (pyrolysis)	1.14 (N_2)

Table 2
Simulations conditions.

Simulation	Studied parameter	Kind of biomass	Steam rate, X_{vap} ($kg_{steam}/kg_{biomass}$)	Pressure, P (atm)	Temperature, T (°C)
S1	Temperature	$CH_{1.36}O_{0.67}$	0	1	600–1000
S2	Temperature		1	1	600–1000
S3	Steam partial pressure		0–2	1	800
S3′	Steam partial pressure + Temperature		0–2	1	600, 800 and 1000
S4	Pressure		1	0–20	800
S5	Kind of biomass	$CH_{1.45}O_{0.67}$	0	1	700–1000

calculations. It goes down from 3 to 1.5 between 650 and 800 °C. This difference shows the importance of water–gas shift reaction (Eq. (5)) in thermodynamic predictions. Effectively, this endothermic reaction is affected by a temperature increase (Le Chatelier's principle).

4.1.2. Comments about wet gas composition

The molar contents of the wet gas mixture are reported in Fig. 5a, and the char rate is reported in Fig. 5b. Both have been evaluated by the thermodynamic equilibrium calculations between 550 °C and 1000 °C. From those two figures, we can notice the following observations:

- A sharp decrease of CO_2 fraction (from 23% down to 0%), of steam fraction (from 30% down to 0%), of CH_4 fraction (from 10% down to 0%) and of char rate (from 60% down to 30%).
- An increase of H_2 and CO fractions (respectively 30–50% and 10–50%).
- The char rate only decline between 550 and 800 °C.

Those results show that the temperature influence on char gasification (Eq. (1)) and Boudouard reaction (Eq. (2)) becomes significant only above 600 °C. The evolution of the gas mixture composition may be explained by the competition between the following reactions (Eqs. (1), (2), (4) and (5)).

As we see in Fig. 5, the char rate and the composition of the gas mixture are constant above 850 °C, because the reactants fractions of Eqs. (1) and (5), steam and CO_2, have reach zero.

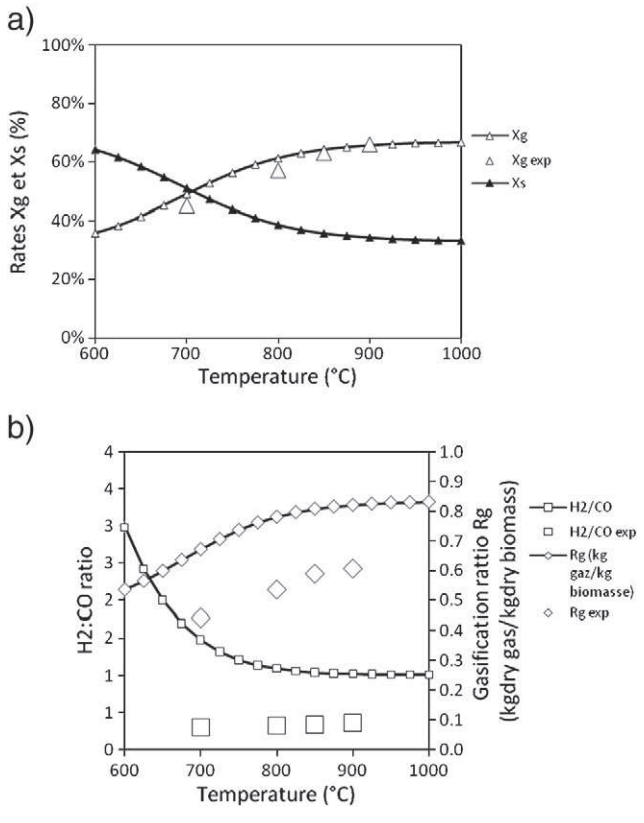

Fig. 3. Pyrolysis efficiency parameters vs temperature (X1 and S1). a) Gasification rate X_g and Char rate X_s, b) H_2: CO ratio and Gasification ratio R_g.

4.2. Steam gasification: Influence of the kind of fluidizing media ($X_{vap} = 1\ kg_{steam}/kg_{dry\ biomass}$)

Experiments X2, X3 and X4 have allowed studying oak steam gasification while using three different solid materials as fluidizing media: sand, alumina, and Nickel catalyst on alumina. Those results have been compared to the predictions of thermodynamic equilibrium state calculations (S2).

4.2.1. Gasification rate and ratio

The comparison of experimental and theoretical gasification rate (X_g) and gasification ratio (R_g) are presented in Fig. 6. The equilibrium gasification rate reaches 100% above 600 °C. This allows assuming the char gasification reactions may happen at moderate temperatures (Fig. 6a). According to the experimental results, obtaining this rate in the reactor would require an excessive residence time of char.

Experimental results (Fig. 6a) show that increasing temperature allows the system getting close from the equilibrium state ($X_g = 97\%$ at 850 °C with Ni/alumina catalyst). Moreover, the use of Ni/alumina catalyst allows obtaining at significantly lower temperatures the same efficiency as the one obtained by using sand particles as fluidizing media (the required temperature decreases about around 150 °C).

The equilibrium gasification ratio (Fig. 6b) slightly declines from 1.5 down to 1.4 $kg_{dry\ gas}/kg_{dry\ biomass}$ between 700 and 900 °C. This is due to

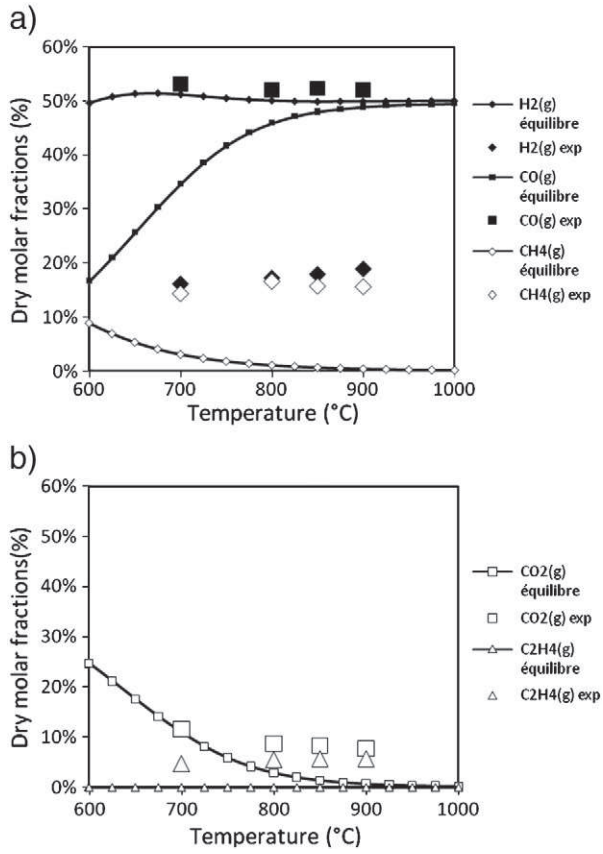

Fig. 4. Pyrolysis gases dry molar fraction pyrolysis vs temperature (X1 and S1). a) H_2, CO and CH_4, b) CO_2 and C_2H_4.

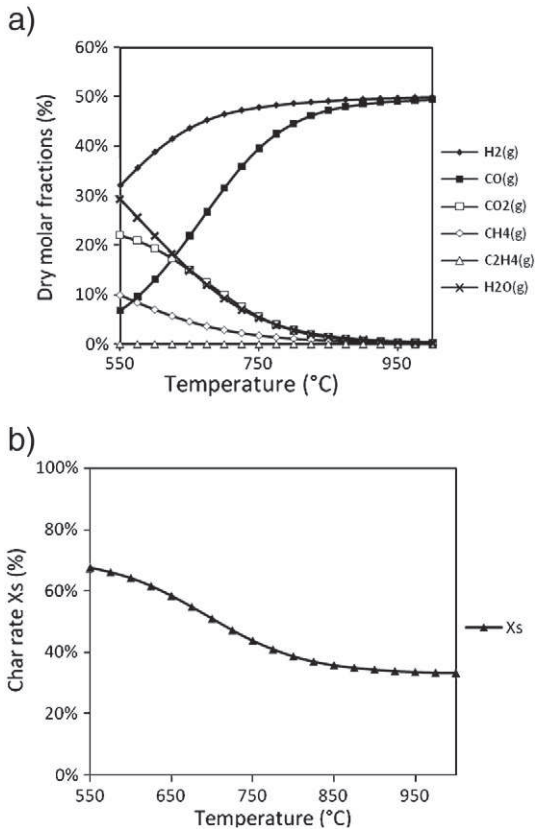

Fig. 5. Pyrolysis gases wet molar fractions and char rate vs temperature (X1 and S1). a) Pyrolysis gases wet molar fractions, b) Gasification char rate.

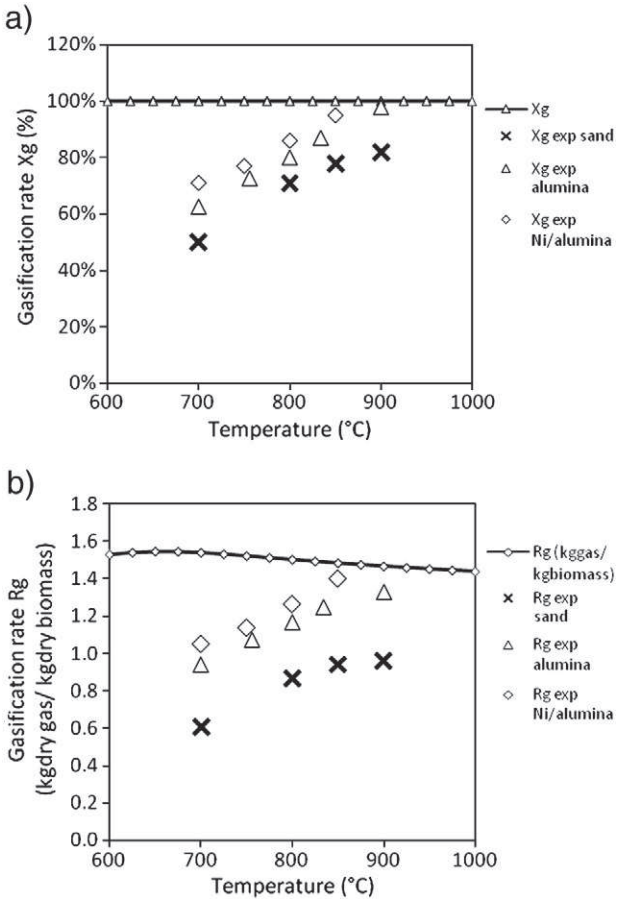

Fig. 6. Gasification rate and gasification ratio vs temperature (X2, X3, X4 and S2). a) Gasification rate X_g, b) Gasification ratio R_g.

the shifting of the water–gas shift reaction (Eq. (5)), penalized at high temperatures. In the actual case, we can notice an opposite trend: the gasification ratio increases with temperature. It corroborates the importance of Eqs. (1) and (2) at high temperatures, generating an increase of the quantity of produced gas. At 850 °C, the gasification rate obtained with the use of Ni/alumina catalyst is even extremely close from the equilibrium state ($R_g = 1.4\ kg_{dry\ gas}/kg_{dry\ biomass}$).

4.2.2. Gas mixture composition

The experimental and theoretical results obtained for each component of the dry gas mixture (H_2, CO, CO_2, CH_4, and C_2H_4) are reported in Fig. 7.

We can notice that the equilibrium gas composition trend is corresponding to the one obtained with pyrolysis. The differences are probably due to the temperature increase, shifting Eqs. (1) and (2) towards H_2 and CO formation, yet a fraction of H_2 produced by Eq. (1) is consumed by reverse water–gas shift (Eq. (5)): the reaction equilibrium is shifted towards CO and H_2O production at high temperatures. This is why H_2 fraction increases for moderate temperatures (beyond 700 °C) and then slightly decreases for high temperatures (Fig. 7a).

The CH_4 fraction decrease may be explained by the promotion of endothermic reactions consuming methane: cracking and steam reforming (Fig. 7d).

The comparison between experimental and theoretical results shows that when the fluidizing media are composed of sand particles, experimental results are very different from simulation predictions, except for CO_2 for which the results are close. Considering the experimental results, we can notice that there is a quantity of hydrocarbons which cannot be neglected, yet there is not any hydrocarbons remaining at the thermodynamic equilibrium state calculation for high

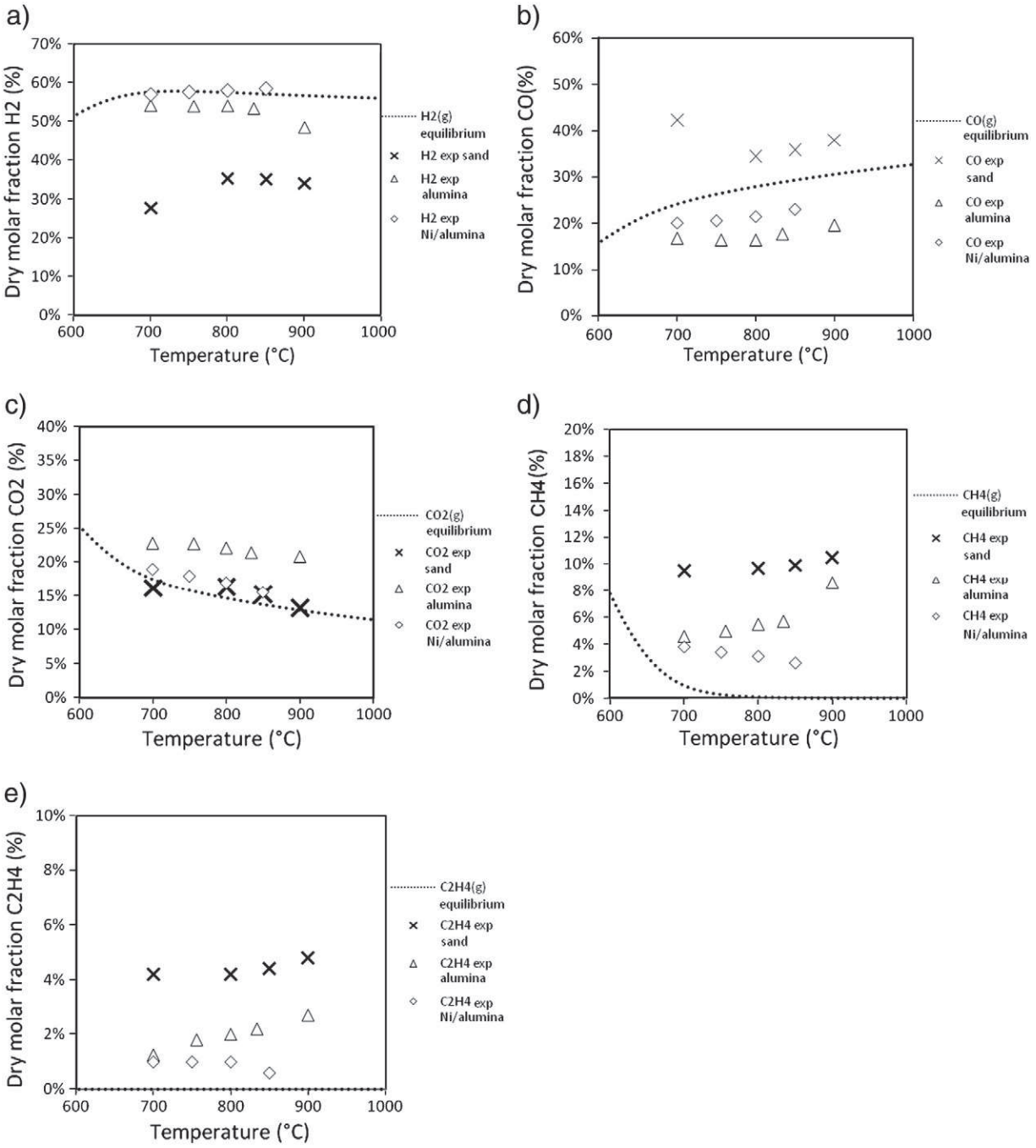

Fig. 7. Gasification gases dry molar fraction vs temperature (X2, X3, X4 and S2). a) H_2, b) CO, c) CO_2, d) CH_4, e) C_2H_4.

temperatures (Figs. 7d and e). We may therefore conclude that they are unsteady, and that their residence time in the reactor may be not long enough to ensure their consumption.

The use of alumina or Ni/alumina catalyst as the fluidizing media promotes H_2 and CO forming, although the fractions of CO, CH_4 and C_2H_4 decrease comparing with the results on sand

Table 3
Comparison of incondensable gases molar fractions depending on the fluidizing media.

	H_2		CO		CO_2		CH_4		C_2H_4	
Equilibrium	58%		28%		15%		0%		0%	
	H_2		CO		CO_2		CH_4		C_2H_4	
	Actual value	Gap	Actual value	Gap	Actual value	Gap	Actual value	Gap	Actual value	Gap
Sand	35%	23%	35%	7%	16%	1%	10%	10%	4%	4%
Alumina	54%	4%	16%	12%	22%	7%	6%	6%	2%	2%
Ni/alumina	58%	0%	21%	7%	17%	2%	3%	3%	1%	1%

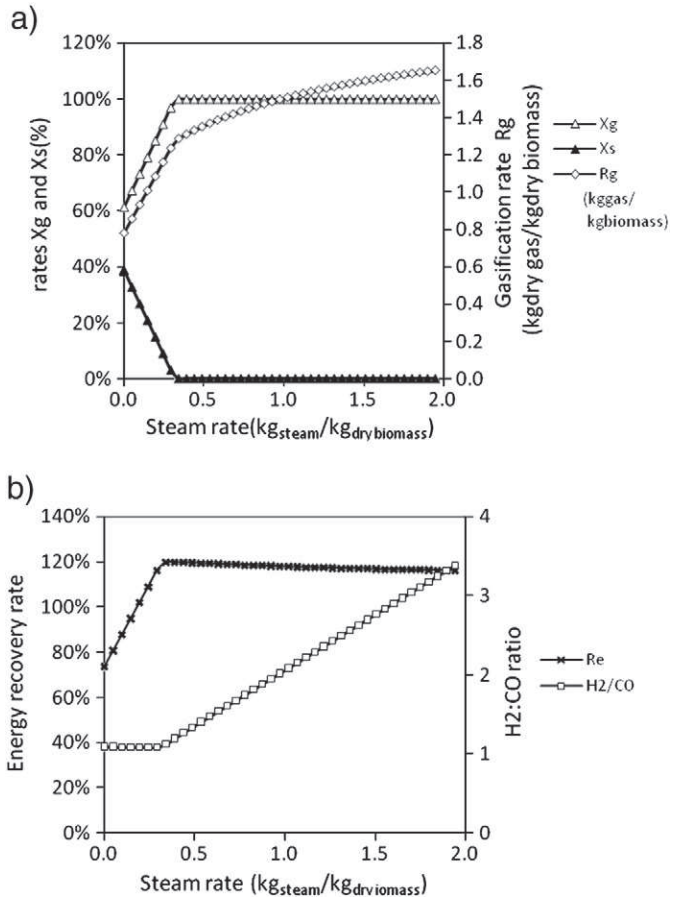

Fig. 8. Gasification efficiency parameters vs X_{vap} (S3).

particles. Water–gas shift reaction (Eq. (5)) and hydrocarbons vapocracking have so to be catalyzed by alumina or Ni/alumina presence.

The actual and theoretical composition of the syngas is gathered in Table 3. Results obtained on Ni/alumina are very close from the thermochemical equilibrium (average difference: 2.6%).

4.2.3. Steam ratio influence (X_{vap})

The gasification rate (X_g), the gasification ratio (R_g) and the char rate (X_s) versus steam rate X_{vap} (simulation S3) are shown in Fig. 8a. The energy recovery rate (R_e) and the H_2: CO ratio are shown in Fig. 8b. The trend of the gasification rate and the char rate between 0 and 0.4 $kg_{steam}/kg_{dry\ biomass}$ emphasizes the steam partial pressure influence on char gasification reaction (Eq. (1)). Between those two values of X_{vap}, the gasification rate raises from 67% up to 100% and the char rate drops from 33% down to 0% when there is enough steam in order to consume completely the char of the reactor. We will designate the steam rate corresponding to the complete consumption of char as the "critical steam rate, X_{vapc}".

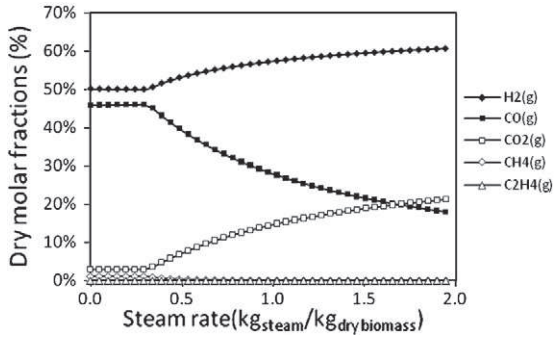

Fig. 9. Gasification gases dry molar fractions vs X_{vap} (S3).

Fig. 9 represents the evolution of dry gas mixture composition versus X_{vap}. We can notice that between 0 and X_{vapc}, the gas mixture composition is constant. The gas composition is equally distributed between H_2 and CO, since the introduced steam is essentially consumed by reaction (Eq. (1)). This phenomenon explains the trend of the energy recovery rate (R_e) of the reactive system, which increases linearly with steam ratio between 0 and X_{vapc} (Fig. 8b).

For steam ratios above X_{vapc}, since the char is completely consumed, the introduction of excessive steam leads to increase its partial pressure, which finally causes the shifting of water–gas shift reaction (Eq. (5)) towards hydrogen production.

Fig. 8b shows that the steam rate is a satisfying parameter to control H_2:CO ratio, thanks to the water–gas shift reaction (Eq. (5)). It increases from 1 to 2.5 when the steam rate increases from 0.4 to 2 $kg_{steam}/kg_{dry\ biomass}$.

We can observe the combination of temperature's influence and steam rate's influence on the results in figures 20 to 25 (S3′). Fig. 10a shows char rate (X_s) evolution versus steam rate at three temperatures: 600, 800 and 1000 °C. It shows that the value of critical steam rate X_{vapc} decreases when the temperature increases (see Table 4). Char gasification (Eq. (1)) is thus completed for smaller quantities of steam when increasing the temperature. Moreover, Figs. 10b–d show that H_2 and CO molar factions are constant until char is completely consumed. Because H_2 and CO are the reactants of Eqs. (1) and (3), we can conclude that the influence of those two reactions is less significant than char gasification (Eq. (1)) influence between 0 and X_{vapc}.

Two trends may be observed in Figs. 10e and f:

- The effect of steam rate on gasification rate and energy recovery rate is important between 0 and X_{vapc}.
- Its effect is then really less significant above X_{vapc}: low progression for gasification rate and stagnation for energy recovery rate.

Those observations corroborate the fact that above X_{vapc}, the steam rate has an influence only on the incondensable gas mixture composition.

Finally, additional observations may be done about the temperature increase (Figs. 10e and f):

- Between 0 and X_{vapc}, the gasification rate and the energy recovery rate increase with temperature.
- Above X_{vapc}, the gasification rate slightly declinees when temperature raises becausee of the influence of temperature on water–gas shift (Eq. (5)), and the energy recovery rate is constant.

4.2.4. Pressure influence

Fig. 11 represents the influence of the gasification reactor pressure (between 1 and 20 atm) on the thermodynamic equilibrium state (S4). Fig. 11a shows that a pressure gradient leads to a low decrease of gasification ratio (R_g), from 1.5 down to 1.42 $kg_{dry\ gaz}/kg_{dry\ biomass}$. Pressure thus has a weak effect on heterogeneous Eqs. (1), (2), and (3), for which reactants are solid and gas. It does not have an effect on water–gas shift reaction as well, for which there is not any change in the number of moles of gas between the reactants and the products.

Fig. 11b presents the evolution of the wet gas mixture composition on the same range of pressure. We notice a slight decrease of H_2 and CO fractions, in the same time than a slight increase of CH_4, CO_2 and H_2O. The pressure gradient therefore has an influence on the reactions leading to a change of the number of moles of gas between the reactants and the products, such as Eq. (4): pressure allows its shifting towards production of CH_4 and H_2O.

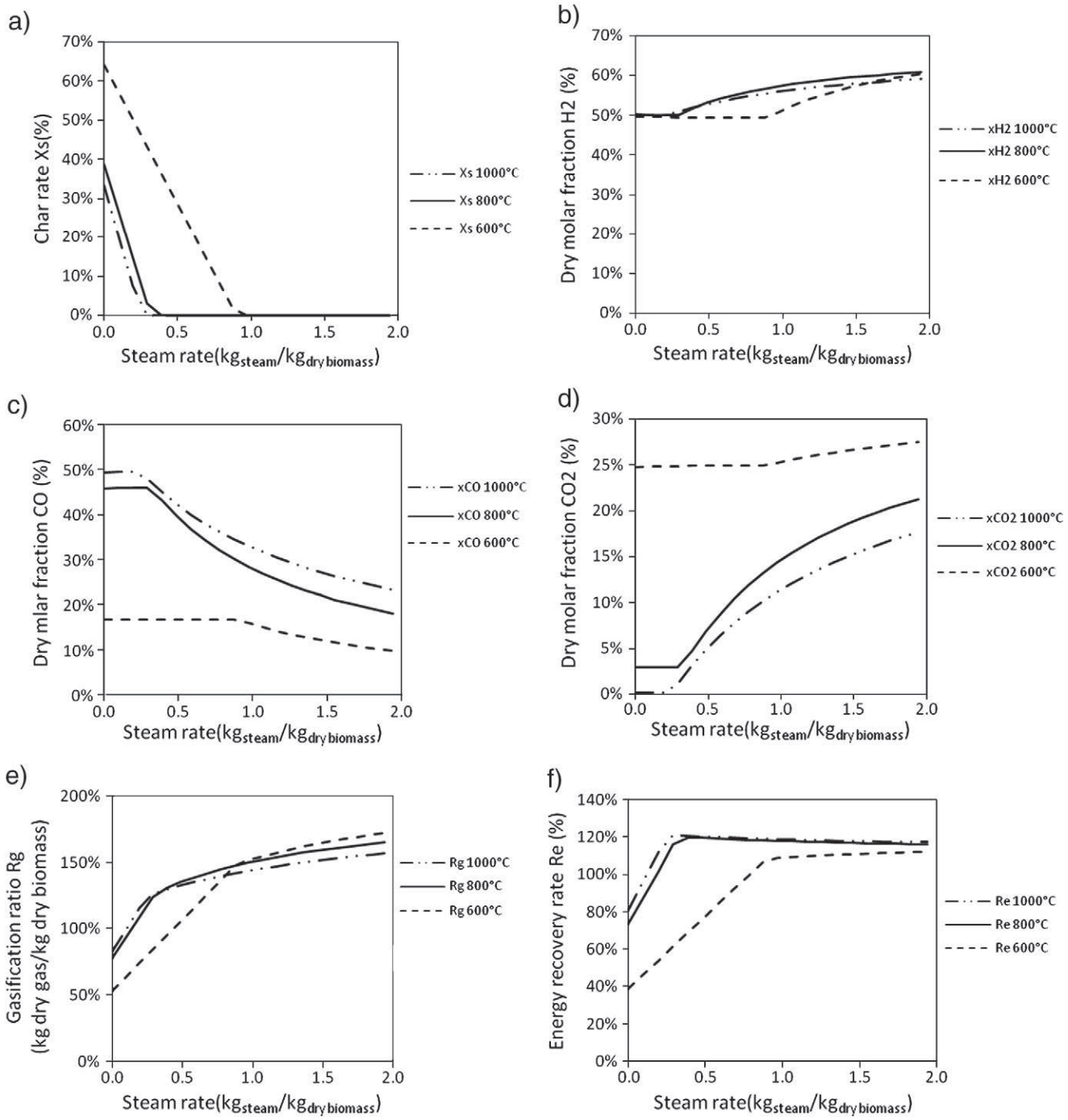

Fig. 10. Gasification parameters vs X_{vap} (S3′). a) Char rate, b) H_2 dry molar fraction, c) CO dry molar fraction, d) CO_2 dry molar fraction, e) Gasification ratio R_g, f) Energy recovery rate R_e.

4.2.5. Kind of biomass influence

In order to study the influence of the kind of biomass used, we have chosen to test two kinds of woods, apparently very different: oak (hardwood) and fir (conifer). Fig. 12 represents the comparison of experimental results (X1) and (X5), with simulations results (S1) and (S5).

Table 4
Critical steam rate versus temperature.

Temperature, T (°C)	600	800	1000
X_{vapc}	95%	40%	35%

The biomass composition analyses have been realized by the Solaize CNRS analysis laboratory. The biomass formulas (oak $CH_{1.36}O_{0.67}$, fir $CH_{1.45}O_{0.67}$) have been confirmed by those observed by the Energy research Centre of the Netherlands [19] (ECN).

It can be noticed that the change of biomass has a very small effect on gasification rate (X_g). The observed difference is smaller than 1%. We may just remark that oak, which has hydrogen content smaller than fir, has the highest gasification rate.

The dry gas mixture obtained by thermodynamic equilibrium state calculations is, in the case studied, completely independent from the kind of biomass used (Fig. 12). The gas mixture composition is exactly

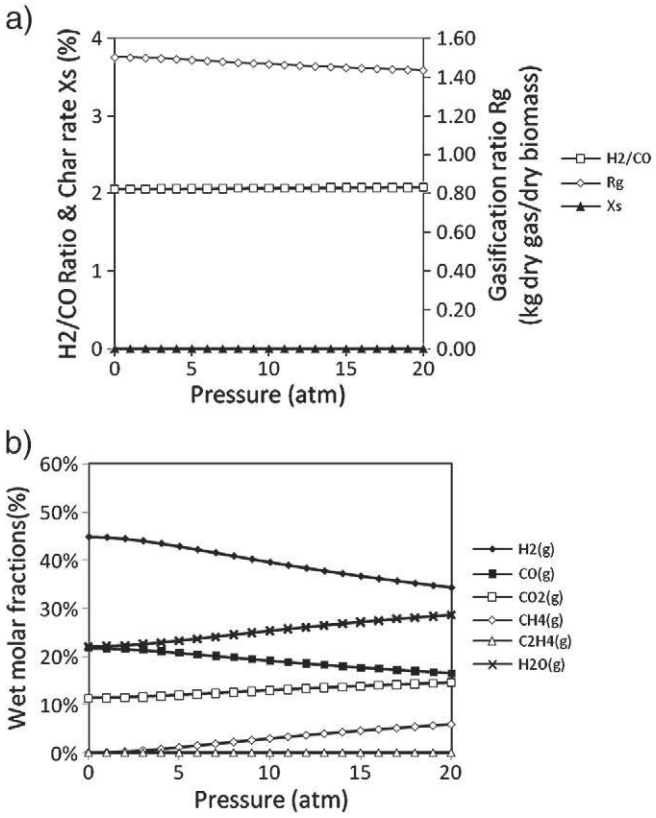

Fig. 11. Gasification results vs pressure (S4). a) Gasification efficiency parameters, b) Gasification gases wet molar fractions.

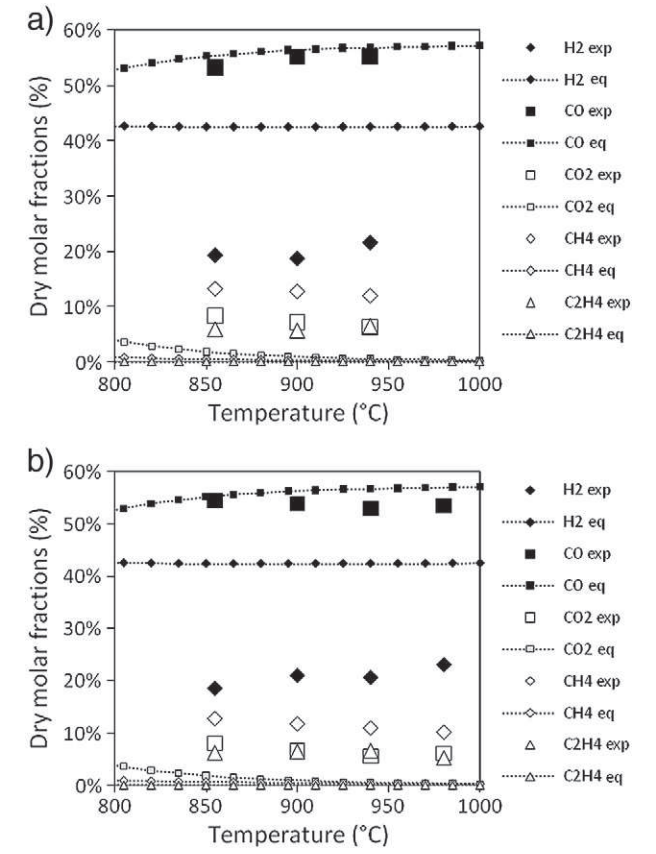

Fig. 12. Pyrolysis gases dry molar fractions vs temperature (X1 and S1). a) Oak, b) Fir.

Table 5
Comparison of dry incondensable gases molar fractions depending on the kind of biomass (pyrolysis).

T (°C)	H_2 (%)		CO (%)		CO_2 (%)		CH_4 (%)		C_2H_4 (%)	
	Oak	Fir	Oak	Fir	Oak	Fir	Oak	Fir	Oak	Fir
855	19.3	18.5	53.2	54.5	8.4	8.0	13.2	12.8	5.8	6.2
900	18.7	21.0	55.2	54.0	7.2	6.7	12.7	11.8	5.6	6.4
940	21.6	20.6	55.3	53.0	6.3	5.5	11.9	11.0	6.4	6.6
980	–	23.1	–	53.5	–	6.0	–	10.2	–	5.2

the same for both kinds of biomass. This similarity is also observed with the experimental results, as shown in Table 5.

5. Conclusions

The thermodynamic equilibrium state calculation of a system initially composed of biomass ($CH_{1.36}O_{0.67}$) and water has been realized in order to evaluate the influence of parameter such as temperature, pressure, relative quantities of water and biomass introduced, and the kind of biomass. Simulation results have been compared to LGC experimental results, obtained in the same conditions.

The steady species which have been observed are: C(s), H_2(g), CO(g), CO_2(g), CH_4(g), H_2O(g).

Simulation results show that the following reactions have a predominant influence.

$$C + H_2O = CO + H_2 \qquad \Delta H_r^0 = 131.3\text{kJ/kmol} \tag{1}$$

$$C + CO_2 = 2CO \qquad \Delta H_r^0 = 172.4\text{kJ/kmol} \tag{2}$$

$$CO + H_2O = CO_2 + H_2 \qquad \Delta H_r^0 = -41.1\text{kJ/kmol} \tag{5}$$

Temperature plays a determinant role on the system efficiency. It promotes endothermic reactions (1) and (2), but penalizes Eq. (5), which is exothermic.

The steam rate (mass of steam introduced per kilogram of dry biomass) does not have an effect between 0 and 0.4 $kg_{steam}/kg_{dry\ biomass}$. Above this threshold, it has a significant effect on the gas mixture composition, since a gradient of steam rate leads to an increase of H_2:CO ratio.

The pressure increase is not promoting the system efficiency.

The kind of biomass (oak or fir) only has a very small effect on experimental and theoretical results.

The experimental results obtained by using a fluidized bed of catalyst particles (Ni/alumina) are very close from the calculations of the thermodynamic equilibrium state.

Acknowledgments

The authors sincerely acknowledge the French Environment and Energy Management Agency (Ademe) and the European Community for funding, and GdF-Suez for managing European GAYA Project in which this work belongs. Special thanks to Bernard MARCHAND and Yilmaz KARA (GdF-Suez).

References

[1] L.K. Mudge, S.L. Weber, D.H. Mitchell, L.J. Sealock, R.J. Robertus, Investigation on catalyzed steam gasification of biomass, Pacific Northwest Laboratory Operated for U.S Department of Energy by Battelle Memorial Institute, 1981.
[2] E.G. Baker, D.H. Mitchell, L.K. Mudge, M.D. Brown, Methanol synthesis gas from wood gasification, Battelle Pacific Northwest Labs, Energy Progress 4 (1983) 226–229.
[3] Chemical Center Lund Institute of Technology, Design Study on Methanol Production for Biomass Fuels, University of Lund, Sweden, 1980.

[4] H. Hofbauer, R. Rauch, G. Loeffler, S. Kaiser, E. Fercher, H. Tremmel, Six years experience with the FICFB-gasification process, 12th European conference and Technology Exhibition on Biomass for Energy, Industry and Climate Protection, 2002.
[5] A. Zschetsche, A. Hofbauer, A. Schmidt, Gasification in an Internally Circulating Fluidized Bed, 8th European Conference on Biomass for Agriculture and Industry, 3, 1994, pp. 1771–1777.
[6] W. Gumz, Gas Producers and Blast Furnaces, Wiley, New York, 1950.
[7] S. Jarungthammachote, A. Dutta, Thermodynamic equilibrium model and second law analysis of a downdraft waste gasifier, Energy 32 (9) (2007) 1660–1669.
[8] Z.A. Zainal, R. Ali, C.H. Lean, K.N. Seetharamu, Prediction of a downdraft gasifier using equilibrium modeling for different biomass materials, Energy Conversion and Management 42 (2001) 1499–1515.
[9] A. Melgar, J.F. Pérez, H. Laget, A. Horillo, Thermochemical equilibrium modelling of a gasyfying process, Energy Conversion and Management 48 (2007) 59–67.
[10] A.K. Sharma, Equilibrium modeling of global reduction reactions for a downdraft (biomass) gasifier, Energy Conversion and Management 49 (2008) 832–842.
[11] C.R. Altafini, P.R. Wander, R.M. Barreto, Prediction of the working parameters of a wood waste gasifier through an equilibrium model, Energy Conversion and Management 44 (2003) 2763–2777.
[12] X. Li, J.R. Grace, A.P. Watkinson, C.J. Lim, A. Ergüdenler, Equilirium modeling of gasification: a free energy minimization approach and it's application to a circulating fluidized bed coal gasifier, Fuel 80 (2001) 195–207.
[13] S. Liu, Y. Wang, L. Wu, J. Oakey, Thermodynamic equilibrium study of trace element transformation during underground coal gasification, Fuel Processing Technology 87 (2006) 209–215.
[14] X.T. Li, J.R. Grace, C.J. Lim, A.P. Watkinson, H.P. Chen, J.R. Kim, Biomass gasification in a circulating bed, Biomass and bioenergy (2004) 171–193.
[15] G. Schuster, G. Löffler, K. Weigl, H. Hofbauer, Biomass steam gasification—an extensive parametric modeling study, Bioresource Technology 77 (2001) 71–79.
[16] M.J. Prins, K.J. Ptasinski, F.J.J.G. Janssen, From coal to biomass gasification: comparison of thermodynamic efficiency, Energy 32 (2007) 1248–1259.
[17] M. Hemati, Etude de la pyrolyse et de la gazéification de bois par thermo-gravimétrie et en lit fluidisé de catalyseur, PhD thesis, Institut National Polytechnique de Toulouse, 1984.
[18] L. El Ghezal, Contribution à l'étude de la pyrolyse et de la vapogazéification de sciure de bois dans un réacteur à lit fluidisé de sable chaud, PhD thesis, Institut National Polytechnique de Toulouse, 1983.
[19] Energy research Centre of the Netherlands, Phyllis, database for biomass and waste, http://www.ecn.nl/phyllis.